

## Size effects in ordered arrays of magnetic nanotubes: Pick your reversal mode

Julien Bachmann,<sup>1,2,a)</sup> Juan Escrig,<sup>2,3</sup> Kristina Pitzschel,<sup>1</sup> Josep M. Montero Moreno,<sup>1,4</sup> Jing Jing,<sup>2</sup> Detlef Görnitz,<sup>1</sup> Dora Altbir,<sup>3</sup> and Kornelius Nielsch<sup>1</sup>

<sup>1</sup>*Institute of Applied Physics, University of Hamburg, 20355 Hamburg, Germany*

<sup>2</sup>*Max Planck Institute of Microstructure Physics, 06120 Halle, Germany*

<sup>3</sup>*Physics Department, Universidad de Santiago de Chile (USACH), 917-0124 Santiago, Chile*

<sup>4</sup>*Electrodeposition and Corrosion Laboratory, University of Barcelona, Barcelona, 08028 Spain*

(Presented 13 November 2008; received 16 September 2008; accepted 7 December 2008; published online 12 March 2009)

Ordered arrays of magnetic nanotubes are prepared by combining a porous template (anodic alumina) with a self-limiting gas-solid chemical reaction (atomic layer deposition). The geometric parameters can thus be tuned accurately (tube length of 1–50  $\mu\text{m}$ , diameter of 20–150 nm, and wall thickness of 1–40 nm), which enables one to systematically study how confinement and anisotropy effects affect the magnetic properties. In particular, the wall thickness of such ordered  $\text{Fe}_3\text{O}_4$  nanotubes has a nonmonotonic influence on their coercive field. Theoretical models reproduce the size effects that are experimentally observed and interpret them as originating from a crossover between two distinct modes of magnetization reversal. © 2009 American Institute of Physics. [DOI: 10.1063/1.3074109]

Structures of submicron dimensions display size- and shape-dependent physical properties when they are small enough with respect to the characteristic correlation lengths of the physical phenomena considered. Magnetism makes no exception to this tenet, and fundamental research into very small magnetic systems is fuelled by their microelectronic and biomedical applications.<sup>1</sup> The physical insight delivered by a magnetic measurement is always contingent upon the quality of the sample—for ensemble measurements, primarily the homogeneity in the size and shape of the particles and their spatial distribution. Because the preparation of nanoparticles with sufficient control over geometry and organization is not trivial, extensive research efforts have focused on the simplest geometry, which is the sphere, defined by a single parameter—its diameter.<sup>2</sup> Wires, which require control of two parameters, diameter, and length, imply more involved preparative strategies, and accordingly, the investigation of their magnetic properties is more recent.<sup>3</sup> This paper presents a synthetic strategy for the large-scale creation of magnetic tubes (a structure with three degrees of freedom: diameter, length, and wall thickness) in hexagonally arranged arrays. We show that in such systems, the ability to systematically tune one geometric parameter while the others are maintained constant delivers unprecedented physical insight.

Our preparative approach combines two aspects. The first is the utilization of ordered porous anodic aluminum oxide as template.<sup>4</sup> This material is obtained by the electrochemical oxidation of aluminum metal under high voltage in an acidic electrolytic solution, and it shows hexagonally arranged cylindrical pores, whose length and diameter are determined (approximately between 0.3 and 300  $\mu\text{m}$ , and between 20 and 200 nm) by the anodization time and voltage,

respectively. The second ingredient of the preparation is a thin film deposition technique applicable to the conformal coating of pore structures with such high aspect ratios—atomic layer deposition (ALD).<sup>5</sup> In ALD, one exposes the substrate surface to two thermally stable molecular precursor gases in alternating fashion; the two precursors only react with each other as adsorbed species on the surface, which results in a monolayer-by-monolayer growth. Thus, the deposition rate does not depend on mass transport phenomena, and inhomogeneities in the partial pressures appearing in the porous structures are irrelevant. The deposited thickness depends on only one easily controlled experimental parameter—the number of cycles of alternated exposures to the precursors. To date, this outstanding level of control achievable by ALD has been applied only minimally toward the preparation of magnetic nanostructures.

We found<sup>6</sup> that thin films of  $\text{Fe}_2\text{O}_3$  can be obtained in ALD mode from either the hydrolysis of iron *tert*-butoxide,  $(t\text{BuO})_2\text{Fe}$ , or the ozone combustion of ferrocene,  $\text{Cp}_2\text{Fe}$ , with similar results; they are smooth and very homogeneously thick. When the reactions are applied to a porous alumina template, tubes are obtained with conformal wall thickness (Fig. 1) up to aspect ratios of approximately 100 (if the hydrolysis is used) and 1000 (with the combustion). The outstanding ability of the procedure to tune the geometry of the tubes appears clearly in the top panel of Fig. 1—changes in wall thickness as subtle as 1 nm can be observed unambiguously by the naked eye, and the intensity of the brown color furnishes an indication of the homogeneity of the deposition over several  $\text{cm}^2$ . After reduction in the brown (semiconducting)  $\text{Fe}_2\text{O}_3$  to black (metallic and ferrimagnetic)  $\text{Fe}_3\text{O}_4$  by  $\text{H}_2$ ,<sup>7</sup> the tubes are poised for systematic investigations into the influence of shape anisotropy over their magnetic properties; not only can their geometry be adjusted at

<sup>a)</sup>Electronic mail: julien.bachmann@physik.uni-hamburg.de.

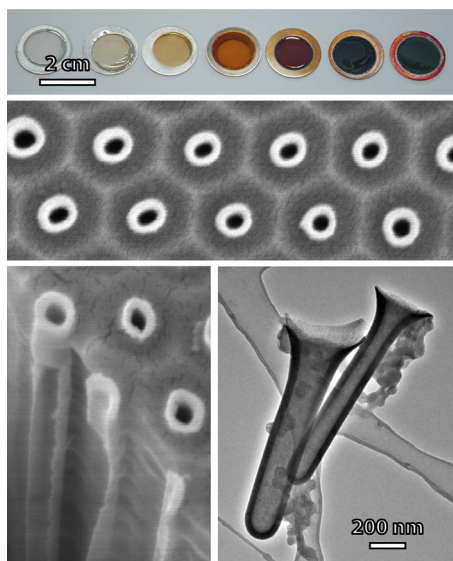


FIG. 1. (Color online) Structure of iron oxide nanotubes. From top to bottom and left to right: photograph of a series of samples of  $\text{Fe}_2\text{O}_3$  tubes in the porous alumina membranes with 50 nm outer diameter and increasing wall thicknesses (0, 1, 2, 4, 8, 12, and 16 nm, respectively); scanning electron micrographs of  $\text{ZrO}_2/\text{Fe}_2\text{O}_3/\text{ZrO}_2$  tubes of 180 nm outer diameter embedded in the matrix, observed in cross section, and at a break of the sample; transmission electron micrograph of short  $\text{Fe}_3\text{O}_4$  tubes of 180 nm diameter. All micrographs are presented on a common scale. Scanning electron microscopy (SEM) samples were prepared by  $\text{Ar}^+$  ion milling of the top of the membrane, a short KOH etch of alumina (serving to bring out the tubes from the matrix and enhance the contrast), and Au sputter—in this context,  $\text{ZrO}_2$  serves as an etch stop layer and prevents the dissolution of  $\text{Fe}_2\text{O}_3$  during SEM sample preparation.

will, their orientation in the applied magnetic field can also be determined easily.

The results of such a systematic study (with a series of samples in which length and outer diameter of the tubes are maintained constant while the wall thickness is varied) are shown in Fig. 2.<sup>8</sup> In the limit of very thin tubes (100 ALD cycles, less than 3 nm of  $\text{Fe}_3\text{O}_4$ , and red curve), the system behaves as a soft ferromagnet with vanishing remanence and

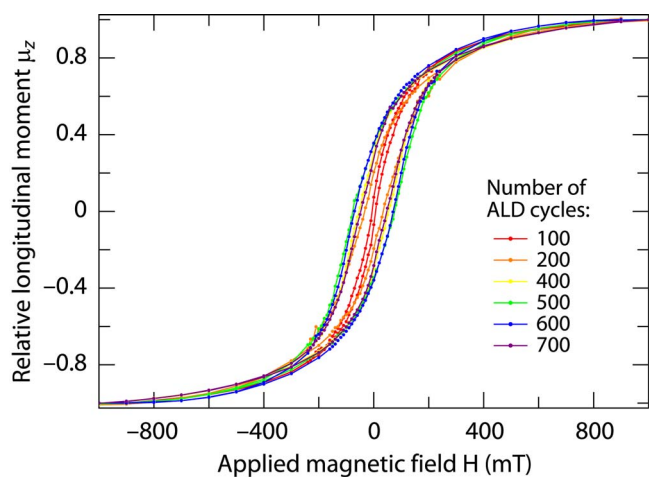


FIG. 2. (Color online) Magnetic hystereses of  $\text{Fe}_3\text{O}_4$  tube arrays (obtained by the reduction in  $\text{Fe}_2\text{O}_3$  prepared by the hydrolysis reaction; 50 nm outer diameter, 105 nm center-to-center distance, and various wall thicknesses  $d_w$  varied between 2 and 18 nm) in porous alumina at 300 K and in a magnetic field  $H$  applied along the tubes ( $z$ ).

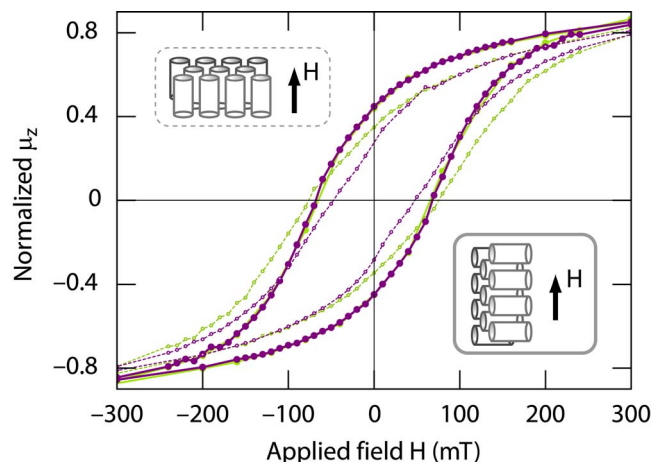


FIG. 3. (Color online) Comparison between the magnetic hystereses of  $\text{Fe}_3\text{O}_4$  nanotube arrays of Fig. 2 in a magnetic field applied perpendicular (solid thick curves) and parallel (thin dashed curves) to the  $z$  axis of the tubes. The light green curves correspond to tubes prepared with 500 ALD cycles and the dark purple ones with 700 cycles.

coercivity. The hystereses widen as the wall thickness  $d_w$  is increased up to 13 nm (500 cycles, green), but after this optimum value, further thickening is accompanied by declining remanence and coercive field. What is more, the geometric dependence observed changes depending on the orientation of the sample with respect to the applied field. As displayed by Fig. 3, when  $H \perp z$ , the hysteresis is constant between  $d_w=13$  nm (light green) and  $d_w=18$  nm (deep purple), which contrasts the observations done with  $H \parallel z$  (shown for comparison in thin dashed lines). This type of behavior usually correlates with strong dipolar interactions between densely packed elongated magnetic objects.<sup>9</sup>

Theoretical models furnish a rationale for the presence of an “optimal” wall thickness (which appears clearly when the orange data points in Fig. 4 are considered) and allow for a quantification of the dipolar interactions between neighboring tubes.<sup>10</sup> As a starting point, we consider the two inhomogeneous magnetization reversal modes that are possible in

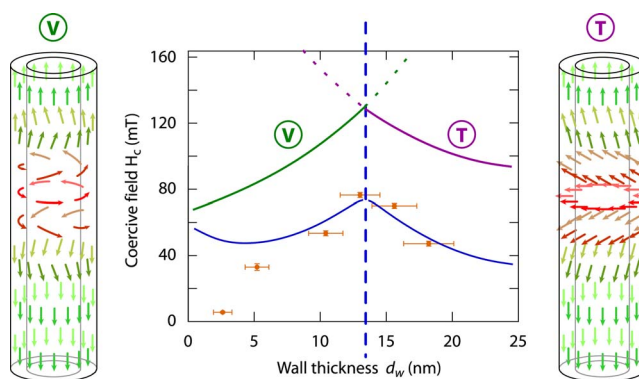


FIG. 4. (Color online) Geometry dependence of the coercive field in the series of  $\text{Fe}_3\text{O}_4$  tube arrays of Fig. 2. Orange points, experimental data; green and purple curves, values computed for isolated tubes reversing their magnetization in vortex (V) and transverse (T) modes, respectively; the reversal modes are schematically displayed on either sides of the graph; solid blue line, curve computed for ensemble of tubes in dipolar coupling with each other; the maximum of the curve virtually separates the graph in two regions (dashed blue line), dominated by either reversal mode.

such systems,<sup>11</sup> which are the vortex (**V**) and transverse (**T**) modes, displayed schematically in Fig. 4. In both modes, a domain boundary appears at one extremity of the tubes and propagates to the other in order to reverse the magnetization from one saturated state to the other, but the organization of the magnetic moments within the domain boundary differs; in **V**, they remain within the wall of the magnetic material, whereas in **T**, a net magnetization component appears in the ( $x, y$ ) plane. One might expect that **V** should be more favorable for thin tubes (which can be approximated by rolled-up films), whereas **T** would dominate thicker tubes, in which the importance of surface effects is lower. This is confirmed by quantitative modeling. Approximating the coercive field generated by **V** with an adapted Stoner-Wolfarth model<sup>12</sup> in which the length of the coherent rotation is replaced by the length of the domain boundary yields the  $d_w$  dependence described by the green curve of Fig. 4, and using the equations of Chang *et al.*<sup>13</sup> for **T** produces the purple curve.<sup>10</sup> The two curves cross at  $d_w \cong 13$  nm, as experimentally observed. Thus, the nonmonotonic dependence of the magnetic properties on geometry can be attributed to a crossover between two different reversal modes. However, the absolute values calculated for the coercive fields of isolated tubes are higher than those measured for the arrayed samples. This discrepancy can be accounted for if the dipolar coupling of each magnetic object to the stray field of the ensemble is considered. Building the effect of stray fields into the model delivers the blue curve of Fig. 4,<sup>10,14</sup> which compares well with the experimental data.

Thus, one can design tubes that will reverse their magnetization by either the vortex or the transverse mode simply by properly adjusting their geometric parameters outer diameter and wall thickness (for a given material). Alternatively, one can maximize their coercive field by choosing a geometry at which the crossover between **V** and **T** takes place. Such control and predictive power could prove useful for future applications. It also raises more fundamental questions concerning the manipulation of magnetic domain boundaries. For example, magnetic tubes exhibiting modulations in diameter could consist of segments reversing their magnetization via different modes and accordingly at different fields. Such phenomena would result in controlled pinning of domain boundaries. The general preparative method described here, which bases on ALD into a porous anodic alumina template, is applicable to the preparation of such structures in macroscopic arrays.

We thank Prof. S. Mathur and S. Barth for preparing  $(t\text{BuO})_6\text{Fe}_2$  and Dr. M. Knez for his help with TEM. This work was supported by the German Ministry of Education and Research (BMBF Grant No. 03N8701), the German Sci-

ence Foundation (DFG) via the SFB668, Millennium Science Nucleus Basic and Applied Magnetism (Project No. P06-022F), USAFOSR (Award No. FA95550-07-1-0040), and Fondecyt (Grant Nos. 11070010 and 1080300). J.B. acknowledges the Alexander von Humboldt Foundation for a postdoctoral research fellowship (Grant No. 3-SCZ/1122413 STP).

<sup>1</sup>S. Sun *et al.*, *Science* **287**, 1989 (2000); R. H. Koch *et al.*, *Phys. Rev. Lett.* **81**, 4512 (1998); R. P. Cowburn *et al.*, *ibid.* **83**, 1042 (1999); S. A. Wolf *et al.*, *Science* **294**, 1488 (2001); T. Gerrits *et al.*, *Nature (London)* **418**, 509 (2002); D. F. Emerich and C. G. Thanos, *Expert Opin. Biol. Ther.* **3**, 655 (2003).

<sup>2</sup>T. M. Whitney *et al.*, *Science* **261**, 1316 (1993); G. A. Prinz, *ibid.* **282**, 1660 (1998); T. Thurn-Albrecht *et al.*, *ibid.* **290**, 2126 (2000); K. Nielsch *et al.*, *Appl. Phys. Lett.* **79**, 1360 (2001).

<sup>3</sup>V. F. Puentes, K. M. Krishnan, and A. P. Alivisatos, *Science* **291**, 2115 (2001); J. P. Chen, C. M. Sorensen, K. J. Klabunde, and G. C. Hadjiapanayis, *Phys. Rev. B* **51**, 11527 (1995); T. Hyeon, *Chem. Commun. (Cambridge)* **8**, 927 (2003).

<sup>4</sup>H. Masuda and K. Fukuda, *Science* **268**, 1466 (1995); K. Nielsch *et al.*, *Nano Lett.* **2**, 677 (2002).

<sup>5</sup>R. L. Puurunen, *J. Appl. Phys.* **97**, 121301 (2005); M. Knez, K. Nielsch, and L. Niinistö, *Adv. Mater. (Weinheim, Ger.)* **19**, 3425 (2007).

<sup>6</sup>Self-ordered anodic alumina membranes were prepared as conventional in two steps, in home-built electrochemical setups (Ref. 4). Arrangements of pores with 50 nm diameter and 105 nm period were obtained at 8 °C under 40 V in 0.3 mol/L oxalic acid and samples with 180 nm diameter and 460 nm period at 1 °C under 196 V in 1% phosphoric acid. Deviations from the nominal geometric parameters are on the order of 10%. We then investigated two chemical reactions toward ALD of  $\text{Fe}_2\text{O}_3$  in a Cambridge Nanotech reactor: hydrolysis of the iron tris(*tert*-butoxide) dimer at 140 °C and ozone combustion of ferrocene at 200 °C [ $(t\text{BuO})_6\text{Fe}_2 + \text{H}_2\text{O}$  and  $\text{Cp}_2\text{Fe} + \text{O}_3$ ]. The former reaction yields a growth rate of approximately 0.25 Å/cycle; the latter yields 0.2 Å/cycle. We observed that deposition of 5 nm  $\text{Al}_2\text{O}_3$ ,  $\text{SiO}_2$ , or  $\text{ZrO}_2$  by ALD before and/or after  $\text{Fe}_2\text{O}_3$  does not affect the tubes. The  $\text{Fe}_2\text{O}_3$  material was converted to  $\text{Fe}_3\text{O}_4$  by treatment under 5%  $\text{H}_2$ /95% Ar at 400 °C for 12 h.  $\text{Fe}_3\text{O}_4$  tubes were protected from aerobic reoxidation by either a 5-nm thick  $\text{SiO}_2$  ALD layer or a macroscopic film of polystyrene applied under  $\text{N}_2$ . Superconducting quantum interference device measurements were carried out at 300 K on an MPMS-XL magnetometer by Quantum Design. A paramagnetic contribution was manually subtracted from the hysteresis curves.

<sup>7</sup>X-ray photoelectron spectroscopy analysis as well as the saturated magnetization values measured for thin films are consistent with the composition  $\text{Fe}_3\text{O}_4$ . The saturated magnetization of Fe is 70% larger (on a per mol of Fe basis) than that of  $\text{Fe}_3\text{O}_4$ . Indeed, in a control experiment we were able to increase the measured saturated magnetization beyond the value of  $\text{Fe}_3\text{O}_4$  by over-reduction in  $\text{H}_2$ /Ar at 450 °C.

<sup>8</sup>J. Bachmann *et al.*, *J. Am. Chem. Soc.* **129**, 9554 (2007).

<sup>9</sup>R. Hertel, *J. Appl. Phys.* **90**, 5752 (2001); M. Hwang *et al.*, *ibid.* **87**, 5108 (2000); H.-J. Jang *et al.*, *Appl. Phys. Lett.* **86**, 023102 (2005); T. G. Sorop *et al.*, *Phys. Rev. B* **67**, 014402 (2003); J. I. Martin *et al.*, *J. Magn. Magn. Mater.* **256**, 449 (2003).

<sup>10</sup>J. Escrig, J. Bachmann, J. Jing, M. Daub, D. Altbir, and K. Nielsch, *Phys. Rev. B* **77**, 214421 (2008).

<sup>11</sup>P. Landeros *et al.*, *Appl. Phys. Lett.* **90**, 102501 (2007).

<sup>12</sup>E. C. Stoner and E. P. Wohlfarth, *Philos. Trans. R. Soc. London, Ser. A* **240**, 599 (1948); *IEEE Trans. Magn.* **27**, 3475 (1991).

<sup>13</sup>C.-R. Chang, C. M. Lee, and J.-S. Yang, *Phys. Rev. B* **50**, 6461 (1994).

<sup>14</sup>M. P. Sharrock *et al.*, *J. Appl. Phys.* **76**, 6413 (1994); P. Allia *et al.*, *Phys. Rev. B* **64**, 144420 (2001).